Compact Substrate Integrated Waveguide Band-pass Rat-race Couplers Based on Mixed Shape Cavity with Flexible Port Topology

Zhigang Zhang, Yong Fan, and Yonghong Zhang

Fundamental Science on Extreme High Frequency Key Laboratory
University of Electronic Science and Technology of China, Chengdu 611731, China
freemanzzg@163.com, yfan@uestc.edu.cn, zhangyhh@uestc.edu.cn

Abstract ─ A new type of compact band-pass rat-race couplers with flexible port topology based on mixed shape substrate integrated waveguide (SIW) cavity is first proposed in this paper. Moreover, composite right/left-handed (CRLH) SIW unit loaded on the common wall between cavities is used to achieve negative coupling structure. The diameter of the vias on the common wall related CRLH-SIW unit is also used to adjust the electric coupling strength and increase the coupling bandwidth. The detailed analysis and the design method have been introduced to realize a filtering rat-race coupler based on substrate integrated fan-shaped cavity (SIFC) and rectangular cavity (SIRC). In particular, the combination of mixed shape resonators and port location in rectangular resonators can be selected according to the requirement of port angle interval. Compared with other filtering couplers, the proposed designs exhibit good filtering responses, high *Q* factor, better isolation, multiple port angle intervals, amplitude balance, as well as 0° and 180° phase differences.

Index Terms ─ Band-pass coupler, flexible port topology, mixed shape cavity, negative coupling structure, substrate integrated fan-shaped cavity (SIFC).

I. INTRODUCTION

Rat-race couplers are essential components in transceivers for microwave communication systems. Miniaturized couplers with high performance are usually required in many applications. As a promising candidate for modern wireless transceiver systems, SIW technology [1-8] is beneficial to the realization of miniaturized couplers and filters due to the fact that it provides an excellent trade-off between waveguide and planar technologies. In [2], synthesis and design techniques of dual-band filters are proposed. A compact multilayer dual-mode filter based on the substrate integrated circular cavity (SICC) is developed in [6].

To further reduce size, a single device integrated with different functionalities, such as filtering coupler [9-21], has been attracting increasing attention. It also recommends an effective way to avoid the performance degradation due to a cascade connection of two individual components. Bandpass 90° and 180° directional couplers with coupled resonators have been first proposed in [9]. A compact filtering 180° hybrid is presented in [12]. Moreover, it is noteworthy that the coupler topologies also have an important impact on the miniaturization of the microwave system. Therefore, the port of the components should be placed at proper positions to meet the requirement of system topology and interconnect.

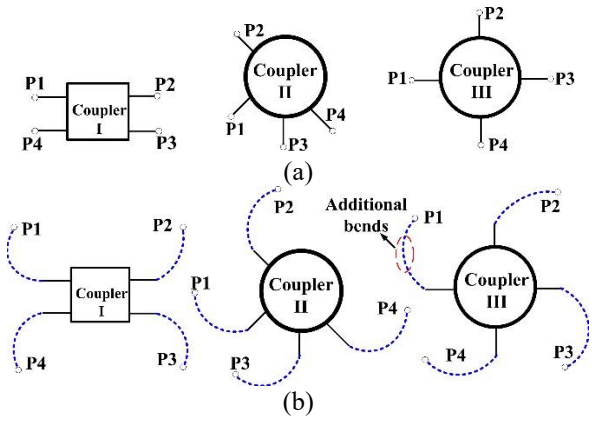

Fig. 1. (a) Different types of topologies of existed couplers, and (b) additional bends are employed to match with the desired transmission direction.

Recently, as shown in Fig. 1 (a), the existed couplers have several different types of topologies. 1) Two ports are placed at one side, and others are placed at the opposite side [9-10],[17],[20]; 2) the distance between each two ports is determined by the required electric length [12-15]; 3) ports are mutually orthogonal [18-19]. By using degenerate orthogonal modes of square SIW cavity, a crossover with bandpass responses is designed in [18]. Four TE_{101}-mode square SIW cavities based on multilayer coupling structures are utilized to construct the filtering rat-race coupler [20]. A SIW filtering rat-race coupler based on TE_{102} and TE_{201} orthogonal degenerate modes is proposed in [21].

However, these types of topologies are not enough

Submitted On: December 23, 2019
Accepted On: February 28, 2020

1054-4887 © ACES

in the high-density circuit design. As such, additional bends (Fig. 1 (b)) will be employed to modify their line direction to meet the system requirement, which leads to a large circuit area, a complex configuration and unwanted loss, electromagnetic compatibility (EMC) problem, especially leakage from the discontinuity. Therefore, it is expected that the port angle interval can be selected flexibly according to the topological requirements without introducing additional L-bends.

In this paper, the mixed shape SIW cavities are first proposed to design band-pass rat-race couplers with flexible port topology. Specifically, by using mixed shape cavities, the structure of filtering coupler can be reasonably constructed according to the topology requirements while keeping good performance. With flexible ports arrangement and resonators combination, the coupler's topology is easy to match with the desired transmission direction, which means that there is no need to add additional L-bend and occupy additional area. What's unique about the analysis process of coupler is that the band-pass coupler is divided into two filtering power dividers, then each power divider is divided into two filters respectively, and the influence of the angle intervals between ports on *Q*e is considered in the design of coupler. Afterwards, the equivalent circuit and coupling matrix method are used to evaluate the initial value of design parameters accurately according to the specifications, which is beneficial to accelerate the later optimization design process. Furthermore, the demand of circuit topology has been integrated into design considerations for the first time, which is helpful to meet the requirement of system interconnect and the design of miniaturized structures.

II. ANALYSIS AND DESIGN

A. Configuration

Several four-element coupler topologies are depicted in Figs. 2 and 3 to demonstrate different ways to achieve different port angular intervals.

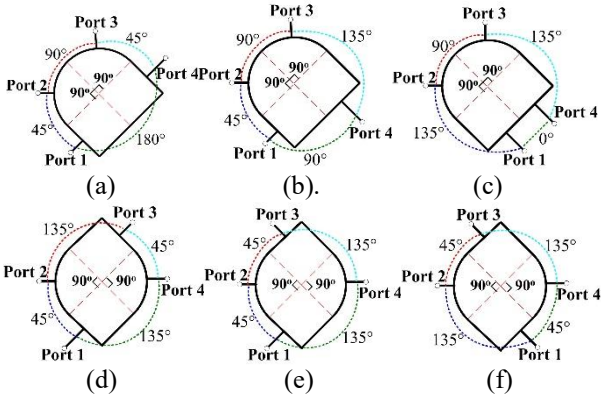

Fig. 2. (a)~(f) Examples of available angular intervals for Type A filtering coupler.

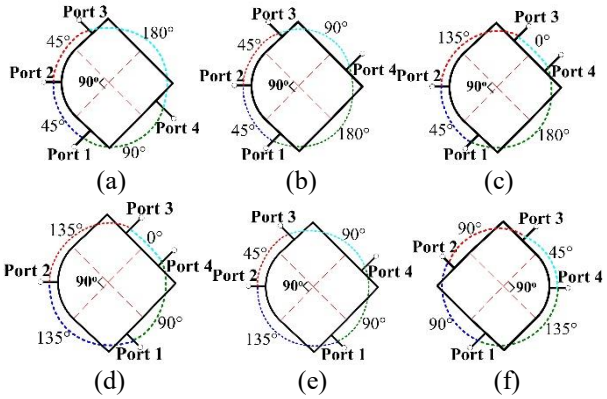

Fig. 3. Examples of available angular intervals for Type B filtering coupler.

The shape of the resonator is very important to obtain the desired port direction while keeping good performance. Rectangular resonators [22-29] are easy to realize 0°, 90° and 180° interval between adjacent ports. Fan-shaped resonators may be a universal configuration. Furthermore, these different shape resonators can be mixed to achieve type A and B couplers with flexible port intervals. The combination of resonators with different shapes and the choice of port location in rectangular resonators are the key factors to construct various angular intervals for input/output ports. Substrate integrated fan-shaped cavities (SIFC) and rectangular cavities (SIRC) are utilized as basic resonance cells of the proposed filtering couplers.

B. Analysis of coupler

The topology of the filtering coupler is shown in Fig. 4 (a). As seen, the rat-race coupler has following two working states. When signals are injected from port 1, the output signals from ports 2 and 4 are in-phase, equal power allocation (M_{21}=M_{41}), just as an in-phase power divider should do. If port 3 is excited, the out-of-phase responses are obtained in ports 2 and 4 (-M_{23}=M_{43}). In this case, the coupler can be seen as an out-of-phase power divider.

As depicted in Figs. 4 (a) and (b), in these two working states, the bandpass coupler is equivalent to an in-phase filtering power divider and an out-of-phase filtering power divider, respectively. Moreover, divider I and II shown in Figs. 4 (b) and (c) are both designed with 3-dB power split ability and have same passband characteristics but quite different phase characteristic. Therefore, the coupling coefficients between resonators of dividers have the following relationship:

$$M_{21}=M_{41}=-M_{23}=M_{43}. \quad (1)$$

In addition, each power divider can be divided into two second-order bandpass filters which have the same operating frequency and passband characteristics, as shown in Fig. 4 (d) ($M_{21,\,BF}$=$M_{41,\,BF}$, $M_{2L,\,BF}$=$M_{4L',\,BF}$).

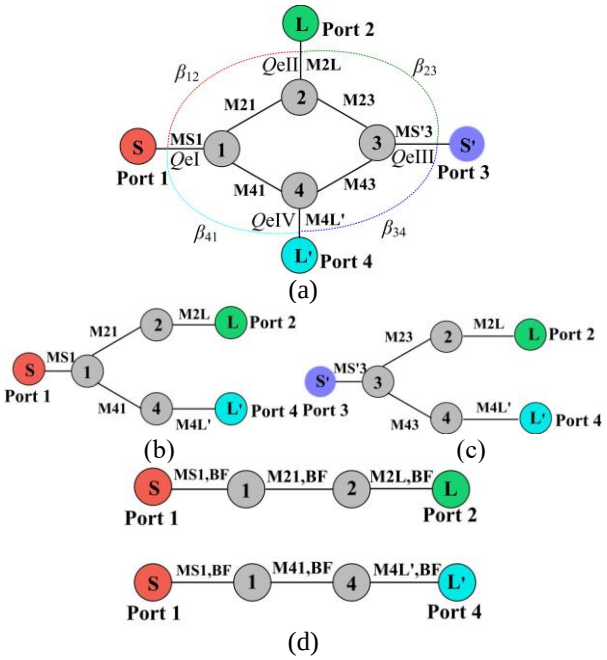

Fig. 4. (a) Topology of the filtering coupler, (b) topology of the filtering in-phase power divider, (c) topology of the filtering out-of-phase power divider, and (d) topology of two second-order filters. Where, β_{12}, β_{23}, β_{34}, and β_{41} are angular intervals for each port, respectively.

Thus, the filtering rat-race coupler can be divided into four bandpss filters. Our strategy is to separately design these four components, and then combine them into one coupler. The coupling matrix of this second-order coupled-resonator band-pass filter is expressed as:

$$m_{N+2}=\begin{array}{c} \\ S \\ 1 \\ 2 \\ L \end{array}\begin{array}{c} \begin{array}{cccc} S & 1 & 2 & L \end{array} \\ \begin{bmatrix} 0 & m_{S1,BF} & 0 & 0 \\ m_{1S,BF} & 0 & m_{12,BF} & 0 \\ 0 & m_{21,BF} & 0 & m_{2L,BF} \\ 0 & 0 & m_{L2,BF} & 0 \end{bmatrix} \end{array}. \quad (2)$$

And the normalized input impedance of the filtering power divider in Fig. 4 (b) is required to be the same as matrix (2). Thus, the coupling coefficients for the filtering power divider topology in Fig. 4 (b) are determined as:

$$M_{S1,BF}=M_{S1}, \quad (3a)$$

$$M_{2L}=M_{4L}=M_{2L,BF}=M_{4L',BF}. \quad (3b)$$

Figure 5 is the equivalent circuit of the filtering coupler. As seen, four parallel *LC* resonators are used to model these four SIW resonators. The in-phase couplings of "resonator 1-to-2" and "resonator 1-to-4" are modeled by two interconnected -90° *J*-inverters (admittance inverters). The 180° out-of-phase couplings of "resonator 3-to-2" and "resonator 3-to-4" are modeled by one +90° and one -90° *J*-inverters, respectively. On the other hand, when port 1 is excited, there are two paths for a signal to reach port 3, one is resonator 1-to-2-to-3 and the other is resonator 1-to-4-to-3. On the first path, there are one "*J*-90°" and one "*J*+90°" inverters so the signal accumulates the phase of 0°. On the second path, there are two "*J*-90°"inverters which lead to 180° accumulated phase. These two signals cancel out each other and result in zero voltage on port3. Thus, isolation between ports 1 and 3 is achieved.

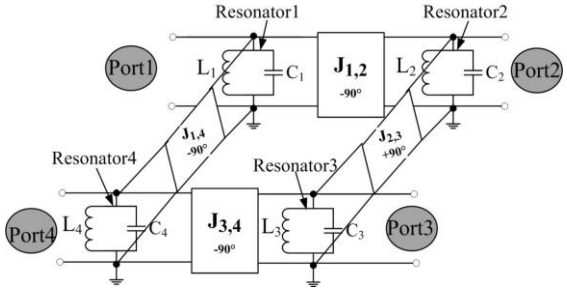

Fig. 5. Equivalent lumped circuit model of the filtering rat-race coupler.

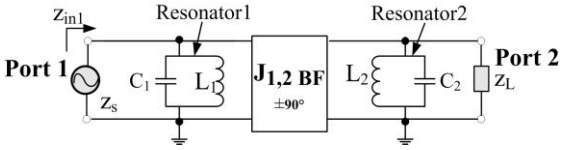

Fig. 6. Equivalent circuit of the coupled-resonator bandpass filter.

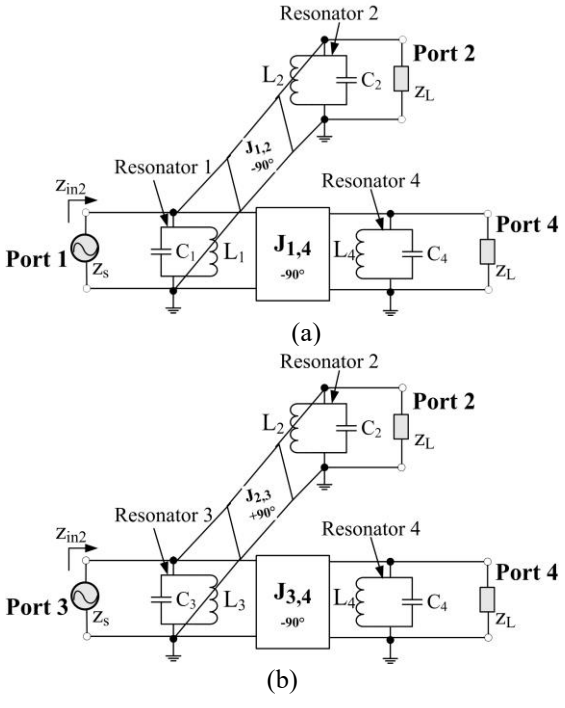

Fig. 7. Equivalent circuit of the filtering power divider: (a) in phase power divider, and (b) out-of-phase power divider.

The cross couplings between "resonator 1-to-3" and "resonator 2-to-4" are neglected in this model because the distances between them are relatively longer. Since the proposed circuit is reciprocal, it can also be excited from port 2 or port 4.Based on the analysis of the above-mentioned topology, the filtering coupler can be seen as consisting of four coupled-resonator filters. The equivalent circuit of the two-order coupled-resonator filter is shown in Fig. 6. The input impedance of this filter is calculated as:

$$z_{in1} = z_s + \frac{j\omega L_1}{1-\omega^2 L_1 C_1} + \frac{\left(j\omega J_{1,2BF}\right)^2}{\frac{j\omega L_2}{1-\omega^2 L_2 C_2} + z_L}. \quad (4)$$

According to the topology of the filtering coupler, the Equivalent circuit of the filtering divider is depicted in Fig. 7. The equivalent circuit of the filtering power divider in Fig. 7 can be realized by adding the nodes "*J*-90°"inverters and resonator 4 to the circuit in Fig. 6. The input impedance of equivalent circuit in Fig. 7 is calculated as:

$$z_{in2} = z_s + \frac{j\omega L_1}{1-\omega^2 L_1 C_1} + \frac{\left(j\omega J_{1,2}\right)^2}{\frac{j\omega L_2}{1-\omega^2 L_2 C_2} + z_L} + \frac{\left(j\omega J_{1,4}\right)^2}{\frac{j\omega L_4}{1-\omega^2 L_4 C_4} + z_L}. \quad (5)$$

In Fig. 5, four resonators are to be designed with the same external quality factor and resonant frequency (L_1= L_2= L_3= L_4=L_0, C_1= C_2= C_3= C_4=C_0). For a 3-dB divider (J_{12}= J_{14}), the input impedance is also given by:

$$z_{in2} = z_s + \frac{j\omega L_1}{1-\omega^2 L_1 C_1} + \frac{\left(j\omega\sqrt{2} J_{1,2}\right)^2}{\frac{j\omega L_2}{1-\omega^2 L_2 C_2} + z_L}. \quad (6)$$

In order to have the same return-loss performance for these two circuits, z_{in1} should be equal to z_{in2}. Based on Eqs. (4) and (6), we have:

$$J_{1,2} = J_{1,4} = \frac{J_{1,2BF}}{\sqrt{2}}. \quad (7)$$

Moreover, the coupling coefficients between resonators [31] are:

$$M_{12} = M_{14} = \frac{J_{1,2}}{\sqrt{\omega_1 C_1 \omega_2 C_2}} = \frac{J_{1,4}}{\sqrt{\omega_1 C_1 \omega_4 C_4}}, \quad (8a)$$

$$M_{12,BF} = M_{21,BF} = \frac{J_{1,2BF}}{\sqrt{\omega_1 C_1 \omega_2 C_2}}, \quad (8b)$$

From Eqs. (7) and (8), the relationship between the coupling coefficients of the filter and the divider is as follows:

$$M_{12} = M_{14} = \frac{M_{12,BF}}{\sqrt{2}}. \quad (9)$$

Based on (1) ~ (3) and (9), the coupling matrix for the filtering power divider topology in Fig. 4 (b) is determined as:

$$M_{S1,BF} = M_{S1}, \quad (10a)$$

$$M_{2L} = M_{4L'} = M_{2L,BF} = M_{4L',BF}, \quad (10b)$$

$$M_{21} = M_{41} = -M_{23} = M_{43} = \frac{M_{21,BF}}{\sqrt{2}} = \frac{M_{41,BF}}{\sqrt{2}}. \quad (10c)$$

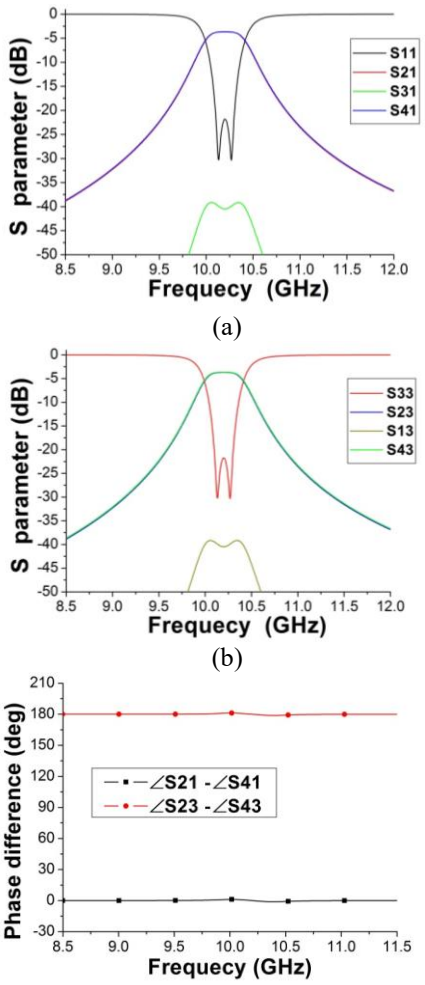

Fig. 8. Circuit simulation of the proposed filtering rat-race coupler: (a) Port1 excited, (b) Port3 excited, and (c) Phase differences.

The required normalized coupling coefficient (m) and external quality factors (Q_e) for the filtering power divider can be calculated by:

$$m_{12} = \frac{M_{21}}{FBW} = \frac{M_{41}}{FBW}, m_{12,BF} = \frac{M_{21,BF}}{FBW}. \quad (11)$$

$$Q_e = \frac{FBW}{M_{S1}^2} = \frac{FBW}{M_{2L}^2} = \frac{1}{FBW \times m_{S1}^2}. \quad (12)$$

Generally, external quality factor (Qe) is related to the following three parameters: the length of feeding slot (Lgap), the width of external coupling aperture (Wc), port angular interval (β). So, the Qe corresponding to

each port of coupler is denoted as: *Q*eI (Wc1, Lgap, β_{12}), *Q*eII (Wc2, Lgap, β_{23}), *Q*eIII (Wc3, Lgap, β_{34}), *Q*eIV (Wc4, Lgap, β_{41}), respectively. In order to obtain the same return loss and passband characteristics on each port, we have:

$$Q\text{eI}= Q\text{eII}= Q\text{eIII}= Q\text{eIV}=Q\text{e}. \quad (13)$$

Since the equivalent circuit in Fig. 6 is a second-order coupled-resonator bandpass filter, it can be design by the conventional synthesis technology [31]. Take the second-order Chebyshev equal-ripple response for example, with the center frequency f_0, ripple level (L_a) (dB), and fractional bandwidth (FBW), and the port admittance Y_0, the element values can be calculated:

$$L=\frac{\sinh(u/4)}{\sqrt{2}}\frac{FBW}{2\pi f_0 Y_0}, \quad (14)$$

$$C=\frac{\sqrt{2}}{\sinh(u/4)}\frac{Y_0}{2\pi f_0\times FBW}, \quad (15)$$

$$J_{1,2BF}=\frac{1}{\sqrt{2}}Y_0\coth(u/4), \quad (16)$$

$$u=\ln[\coth(\frac{\ln 10}{40}\times L_a(dB))]. \quad (17)$$

In this design, a 50-Ω (Y_0=0.02S) filtering rat-race coupler is centered at 10.2 GHz with second-order Chebyshev 0.05-dB equal-ripple response [L_a=0.05(dB)] and 2.6% fractional bandwidth (FBW). Based on above analysis, the filtering coupler can be seen as consisting of four coupled-resonator filters. The parameter values of the equivalent circuits in Fig. 6 and Fig. 7 are then evaluated using (7)–(9),(14)–(17): u=5.85058, L_1= L_2= L_3= L_4=L_0=0.0293nH, C_1= C_2= C_3= C_4=C_0=8.309pF, $J_{1,2\,BF}$=0.01575S, Y_0=0.02S. $J_{1,2}$=$J_{1,4}$=-$J_{2,3}$=$J_{3,4}$=0.0111369S. After determining these parameters, the circuit structure can be constructed to obtain the desired responses.

Figures 8 (a) and (b) show the circuit simulation of the proposed filtering rat-race coupler under the in-phase and out-of-phase operation, respectively. As seen, good filtering responses and amplitude balance can be obtained. Since the whole structure is symmetric, good phase imbalance of less than 1° between ports 2 and 4 is achieved, as shown in Fig. 8 (c).

C. Design consideration

The resonant frequency of mode for circular cavity with solid wall can be calculated by [24],[33]:

$$f_{mpn}=\begin{cases}\dfrac{c}{2\pi\sqrt{\mu_r\varepsilon_r}}\sqrt{\left(\dfrac{\mu'_{mn}}{R}\right)^2+\left(\dfrac{p\pi}{\Delta h}\right)^2} & TE_{mpn}\\ \dfrac{c}{2\pi\sqrt{\mu_r\varepsilon_r}}\sqrt{\left(\dfrac{\mu_{mn}}{R}\right)^2+\left(\dfrac{p\pi}{\Delta h}\right)^2} & TM_{mpn}\end{cases}, \quad (18)$$

where μ_r and ε_r are relative permeability and permittivity of the filling material, μ_{mn} and μ'_{mn} are the nth roots of mth Bessel function of the first kind and its derivative, R is the radius of circular cavity, Δh is the height of the of circular cavity ,and c is the speed of light in free space. According to Eq. (18) and by means of the least square method, the resonant frequency of the TM_{101} mode for SIFC can be calculated by the following formula:

$$f_{101}=\frac{0.383c}{\dfrac{1}{b_\theta}R_{eff}\sqrt{\mu_r\varepsilon_r}},\ R_{eff}=R-\frac{D^2}{0.95p}. \quad (19)$$

Where, θ is the central angle of SIFC, R_{eff} is the equivalent radius of the fan-shaped cavity. D and p are the diameter of metallized via-holes and center-to-center pitch between two adjacent via-holes. b_θ is related to the central angle of a fan-shaped resonator. When θ=45°, 60°, 90°, 120°, b_θ is approximately equal to 3.2, 2.7, 2.1, 1.8, respectively.

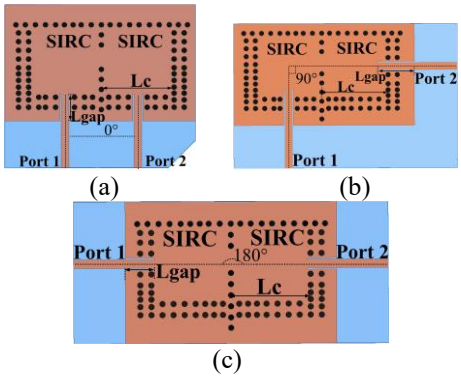

Fig. 9. Several port angular intervals of two SIRCs: (a) 0°, (b) 90°, (c) 180°. Where, *L*c is the side length of the SIRC, *L*gap is the length of feeding slot.

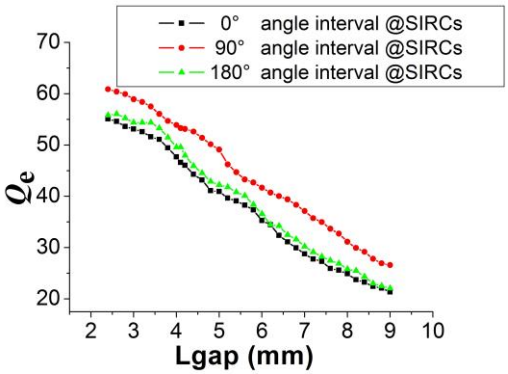

Fig. 10. Extracted *Q*e curves corresponding to different port angle intervals of two SIRCs.

Figure 9 shows the combination of resonators facilitates the acquisition of different port angle intervals and the construction of different coupler topologies. At the same time, however, external quality factor (*Q*e) is also affected by the direction of ports. This means that besides the influence of external coupling parameters on *Q*e, port angle intervals also play an important role.

Therefore, numerical analysis is carried out on SIRCs with microstip lines as its input/output to determine the external quality factor using Ansoft's HFSS. The external coupling is controlled by changing the length of feeding slot (*L*gap) with a fixed feeding slot width.

Figure 10 depicts extracted *Q*e curves versus the length of feeding slot (*L*gap). As we can see, there is little difference between *Q*e variations at 0°and 180° port angular intervals in two SIRCs. When port angular interval is 90°, the value of corresponding *Q*e is larger than that of the previous two cases.

III. FILTERING COUPLER TYPE A

A. Coupler structure

As shown in Fig. 11 (a), the filtering Type A coupler consists of two fan-shaped SIW cavities and two square cavities. The coupling between resonators I and II, I and IV, III and IV is magnetic coupling, which is realized by the iris between the common narrow walls. However, electrical coupling occurs between resonators II and III due to composite right/left-handed (CRLH) transmission line loaded on the common walls.

As shown in Fig. 11 (b), CRLH-SIW unit is achieved by introducing an interdigital slot etched on the metal surface of common post wall of SIW cavities. It should be noted that CRLH-SIW unit is used to achieve negative coupling structure, which decreases the resonant frequency of the corresponding SIW cavities.

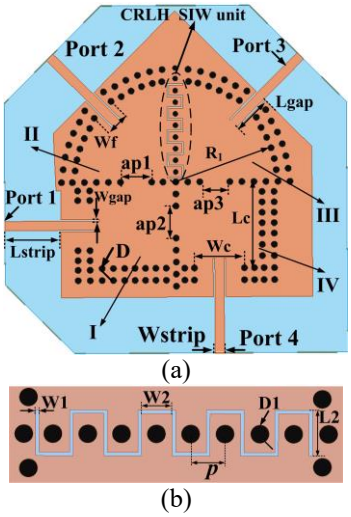

Fig. 11. The proposed Type A filtering coupler: (a) top view and (b) CRLH-SIW unit.

Figure 12 shows the CRLH is loaded on the common walls oure the SIFCs, SIRCs and mixed SIW cavity respectively, resulting in decrease of the central frequency. The main reason is that the negative order resonance is excited in corresponding SIW cavities, which leads to decrease of the cut-off frequency of the waveguide [25]. In addition, the central frequency offset of the SIFCs is larger than that of other cases due to the loading of CRLH, as can be seen from Fig. 12.

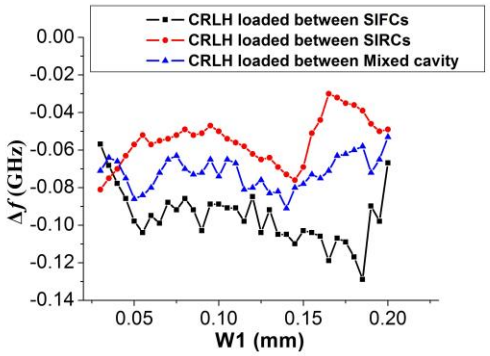

Fig. 12. Variation of the central frequency of SIW cavities with CRLH loaded. Where, $\Delta f=f_1-f_0$, f_1 and f_0 are the central frequency of cavities with and without CRLH loaded, respectively.

B. Design

In our design, the desired passband is centered at 10.2 GHz with the 2.6% fractional bandwidth (FBW) of 19-dB equal-ripple return loss. Based on the advanced coupling matrix synthesis method in [32], the initial normalized coupling matrix of corresponding bandpss filter (BPF) can be synthesized as:

$$m_{N+2}=\begin{array}{c} \\ S \\ 1 \\ 2 \\ L \end{array}\begin{array}{c} \begin{array}{cccc} S & 1 & 2 & L \end{array} \\ \begin{bmatrix} 0 & 1.18591 & 0 & 0 \\ 1.18591 & 0 & 1.57423 & 0 \\ 0 & 1.57423 & 0 & 1.18591 \\ 0 & 0 & 1.18591 & 0 \end{bmatrix} \end{array}. \quad (20)$$

From (7)–(12), (20) the desired parameters of the filtering power dividers can be calculated as follows: $M_{21}= M_{41}= -M_{23}= M_{43}=0.02894$, $Q_{e,S1}=27.3463$, $Q_{e,2L}= Q_{e,4L}=27.3463$. The external quality factor *Q*e is calculated by [31]

$$Q_e=\frac{2f_0}{\Delta f_{3dB}}, \quad (21)$$

where f_0 is the frequency at which S21 reaches its maximum value and Δf_{3dB} is the 3-dB bandwidth for which S21 is reduced by 3 dB from its maximum value.

Figure 13 shows the external quality factor versus the width of the external coupling aperture (*W*c) and the length of feeding slot (*L*gap). It can be seen that the larger the feeding slots length and the external coupling aperture width, the smaller the external quality factor. Based on the previous analysis, the filtering rat-race coupler can be divided into four bandpss filters. The adjustment of external quality factor (*Q*eI, *Q*eII) is realized by changing the value of Lgap, as depicted in

Fig. 13 (a). Then, the desired Qe (QeII = QeIII = Qe) can be achieved and the initial value of Lgap can also be determined. Due to different port angle intervals, the values of QeI and QeIV are greater than that of QeII and QeIII, as can be clearly seen from Fig. 13 (a). Therefore, another external coupling parameter (Wc) needs to be adjusted to achieve the same Qe as Port2 and 3. Figure 13 (b) gives the extracted curve of QeI versus the coupling aperture width Wc, which is determined to meet the requirements with QeI=QeIV=Qe. Thus, the initial value of Wc can be evaluated. Figure 14 illustrates the extracted curves of M_{21} and M_{41}, which versus the coupling iris ap1 and ap2. As can be seen, when the width of the coupling iris increases, coupling coefficients increases accordingly. The coupling coefficients versus the interdigital slot widths (W1) and diameter of the vias (D1) are plotted in Fig. 14. The diameter of the vias on the common wall related CRLH-SIW unit is used to adjust the electric coupling strength and increase the coupling bandwidth. Obviously, smaller W1 and D1 correspond to the wider bandwidth. In summary, the design procedure of the proposed filtering coupler is listed as follows.

Firstly, according to the requirement of the topology structure, the combination of resonators with different shapes can be selected in Fig. 2. Secondly, the resonant frequency of the SIFC is calculated by formula (19), to meet the required center frequency f_0. Thirdly, a coupling matrix of a second-order BPF is synthesized according to the desired center frequency f_0 and the fractional bandwidth (FBW). Fourthly, according to formula (7) ~ (12), the coupling matrix and Qe of the corresponding filtering power divider are obtained. Moreover, internal coupling parameters (ap1, ap2, ap3) and external coupling parameters (Wc, Lgap) are tuned to meet desired values of coupling coefficients and external quality factor, respectively. Finally, fine tuning of the whole structure is performed to realize good filtering coupler performance.

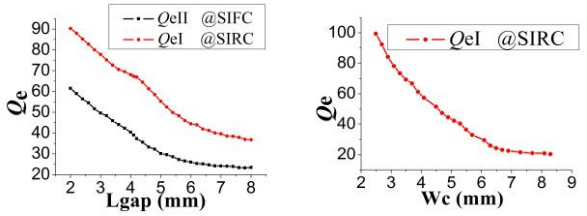

Fig. 13. (a) Simulated external quality factor Qe change with Lgap, Wc=4mm. (b) Simulated QeI change with Wc, Lgap=5mm. Where, QeI=QeIV, QeII=QeIII correspond to port 1, port4 and port2, port3, respectively.

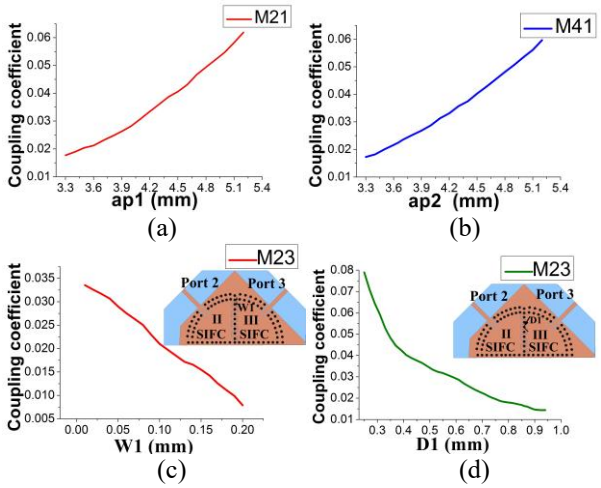

Fig. 14. Coupling coefficients versus the coupling iris: (a) M21 versus ap1, (b) M41 versus ap2, (c) M23 versus W1, and (d) M23 versus D1.

C. Experiment

After optimization implemented by HFSS, the geometry parameters of the proposed coupler are chosen as follows (all in mm): D=0.8, p=1.5, ε_r=3.5, L2=2, W1=0.12, W2=1.35, Wgap=0.2, Lgap=5.1, Wc=6.25, Wstrip =1.15, Lstrip=7, ap1=3.9, ap2=3.95, ap3=3.75, D1=0.59, R_1= 12.63, Lc=10.75, Wf=3.86.

To verify the above method ,the proposed coupler was designed and fabricated on a substrate with thickness of 0.508 mm, relative dielectric constant of 3.5 and dielectric loss tangent 0.0018 (at 10 GHz). The measurement is accomplished by using the Agilent N5244A network analyzer.

Figures 15 (a), (b) shows the simulated and measured S-parameters under the in-phase operation. The measured passband is centered at 10.23 GHz with the 1-dB FBW of 3.5% .The in-band return loss is better than 17.35 dB. The minimum insertion losses including the 3-dB equal power division loss are (3+1.3) and (3+1.35) dB, with the amplitude imbalance of 0.1 dB.

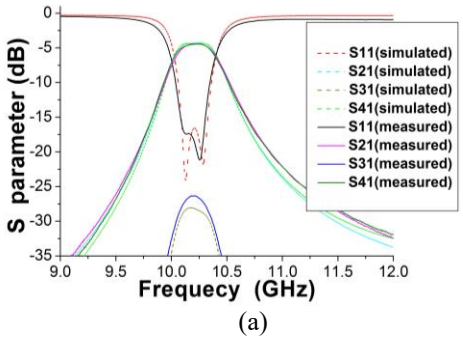

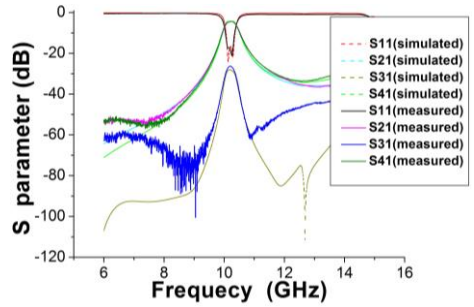

(b)

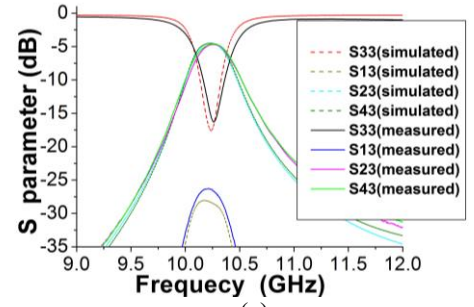

(c)

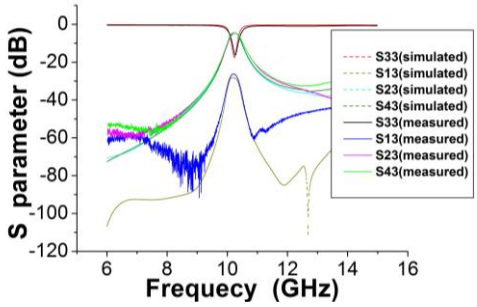

(d)

Fig. 15. Simulated and measured results of the fabricated type A coupler with two SIRCs and two SIFCs (a) and (b) Port 1 is excited, (c) and (d) Port 3 is excited.

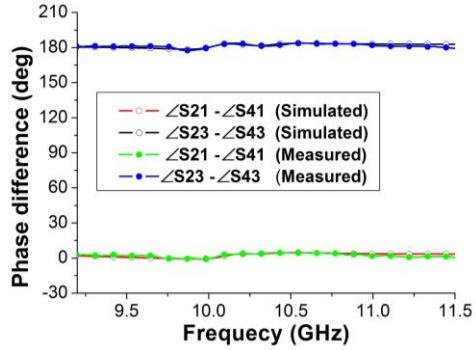

Fig. 16. Phase differences of the fabricated type A coupler.

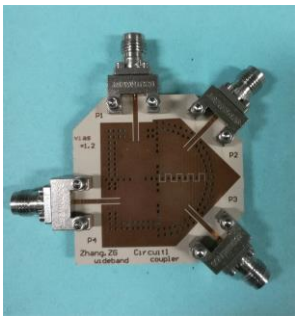

Fig. 17. Photograph of the fabricated filtering type A coupler with two SIRCs and two SIFCs.

The simulated and measured S-parameters under the out-of-phase operation are shown in Figs. 15 (c), (d). The 1-dB FBW of 2.75% is a bit lower than that of the in-phase operation of 3.5%, which is due to the fabrication errors. The insertion losses at the center frequency are (3+1.4) dB and (3+1.45) dB, with the difference of less than 0.1 dB. The measured return loss of port 3 is better than 16.3 dB. In Fig. 15, the isolation between ports 1 and 3 within the passband is better than 26.36 dB, showing high isolation.

When signals are injected from port 1 and port 3, the measured in-band phase differences between two output ports are nearly 0° and 180°, respectively, with the variation of less than 3°, as depicted in Fig. 16. In general, the measured results show good performance of bandpass filtering responses, equal power. Figure 17 is the photograph of the fabricated filtering type A coupler based on two SIRCs and two SIFCs.

IV. FILTERING COUPLER TYPE B

A. Coupler structure

As shown in Fig. 18, the filtering Type B coupler is composed of three square cavities (resonators I~III) and one fan-shaped cavities (resonators IV). In these figures, R_1 is the radius of the SIFC, ap1, ap2 and ap3 are the widths of the coupling iris between the common narrow walls of SIW cavities, *W*c1 and *W*c2 are the width of the external coupling aperture. It should be noted that CRLH-SIW unit is used to achieve negative coupling structure, which decreases the resonant frequency of the corresponding SIW cavities. Therefore, the size of resonators II and III will be smaller than the resonator I (*L*c1<*L*c2).

B. Design

In our design, the desired passband is centered at 10.28 GHz with the 1.5% fractional bandwidth (FBW)

of 20-dB equal-ripple return loss. The initial normalized coupling matrix of corresponding BPF can be synthesized as:

$$m_{N+2} = \begin{array}{c} \\ S \\ 1 \\ 2 \\ L \end{array} \begin{array}{c} \begin{array}{cccc} S & 1 & 2 & L \end{array} \\ \begin{bmatrix} 0 & 1.22474 & 0 & 0 \\ 1.22474 & 0 & 1.65831 & 0 \\ 0 & 1.65831 & 0 & 1.22474 \\ 0 & 0 & 1.22474 & 0 \end{bmatrix} \end{array} \cdot (22)$$

From (7)–(12), (22) the desired parameters of the filtering power dividers can be calculated as follows: $M_{21}= M_{41}=-M_{23}=M_{43}=0.017589$, $Qe,_{S1}=44.4453$, $Qe,_{2L}= Qe,_{4L}=44.4453$. In general, the design procedure of the proposed filtering coupler Type B is listed as follows. First, the combination of resonators with different shapes can be selected in Fig. 3. Second, the resonant frequency of the SIFC is calculated by formula (19). Third, a coupling matrix of a second-order BPF is synthesized according to the desired center frequency f_0 and the FBW. Fourth, according to formula (10) ~ (12), the coupling matrix and Qe of the corresponding filtering power divider are obtained. Moreover, internal and external coupling parameters are tuned to meet desired values of coupling coefficients and external quality factor, respectively. Finally, the optimization is implemented by HFSS and good filtering rat-race coupler performance can be realized.

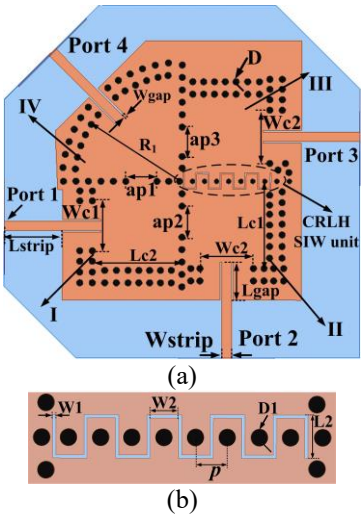

(a)

(b)

Fig. 18. The proposed filtering Type B coupler with three SIRCs and a SIFC: (a) Top view and (b) CRLH-SIW unit.

C. Experiment

To further verify the proposed method, the filtering rat-race type B coupler based on three SIRCs and a SIFC is implemented. The dimensions of the coupler are chosen as follows (all in mm): $L2$=2, $W1$=0.13, $W2$=1.3, Wgap=0.2, Lgap=4.5, Wc1=5.93, Wc2 =6.33, Wstrip =1.15, Lstrip=7, ap1=3.65, ap2=3.65, ap3=3.55, $D1$=0.58, $R1$= 12.9, Lc1=10.53, Lc2=10.77.

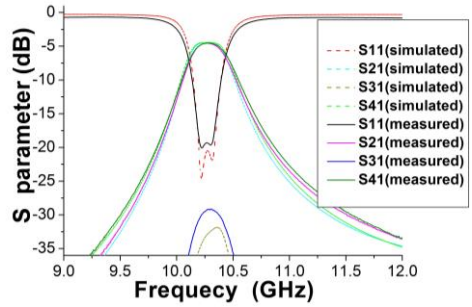

(a)

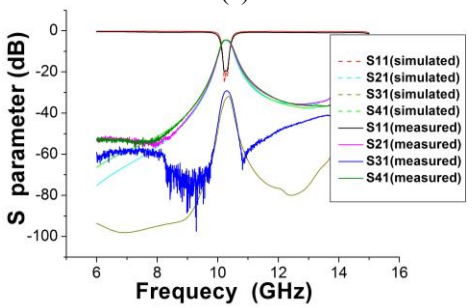

(b)

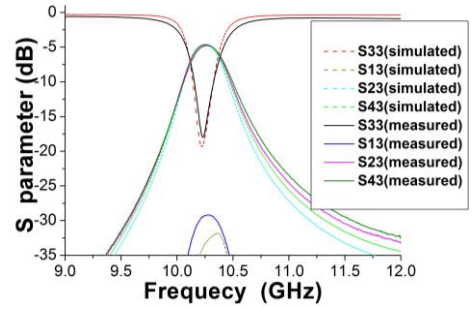

(c)

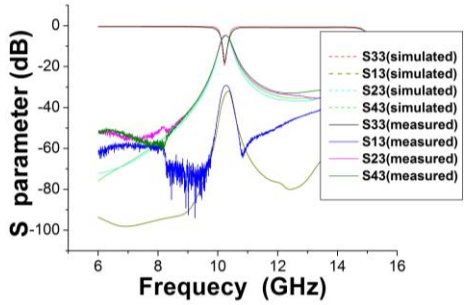

(d)

Fig. 19. Simulated and measured results of the fabricated type B coupler with three SIRCs and a SIFC (a) and (b) Port 1 is excited, (c) and (d) Port 3 is excited.

Figures 19 (a) and (b) shows the simulated and measured results under the in-phase operation. The measured passband is centered at 10.31 GHz with the 1-dB FBW of 2.5%. The minimum insertion losses at the two output ports are (3 + 1.35) and (3 + 1.4) dB, with the

amplitude imbalance of less than 0.1 dB. The return loss is better than 19.3 dB.

Figures 19 (c) and (d) shows the simulated and measured S-parameters under the out-of-phase operation. The measured magnitudes of S23 and S43 are −(3 + 1.4) and −(3 + 1.45) dB, respectively, with the difference of less than 0.1 dB. The measured 1-dB FBW is about 1.9%. The in-band return loss is better than 17.5 dB. As seen, isolation (S31) within the operating frequency band is smaller than −29.6 dB.

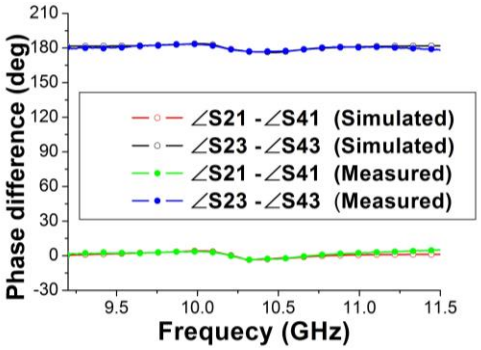

Fig. 20. Phase differences of the fabricated type B coupler with three SIRCs and a SIFC.

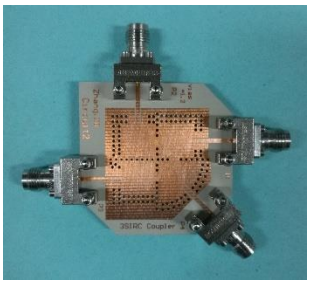

Fig. 21. Photograph of the fabricated filtering type B coupler with three SIRCs and a SIFC.

When signals are injected from port 1 and port 3, the measured in-band phase differences between two output ports are nearly 0° and 180°, respectively, with the variation of less than 3°, as illustrated in Fig.20.

Figure 21 shows the photograph of the fabricated filtering coupler type B based on a SIFC and three SIRCs. A detailed performance comparison with filtering couplers in recent years is shown in Table 1. Compared with [12] and [13], the proposed designs have much higher Q factors and self-consistent electromagnetic shielding structure. By using multilayer structures, the circuits in [20] realize smaller size. However, the multilayer structure is more complex, which increases the difficulty in fabrication and thus increases the processing cost. A filtering rat-race coupler based on the orthogonal modes is proposed in [21]. The desired 0° and 180° phase differences are realized by the inherent characteristics of TE_{102} and TE_{201} modes. Therefore, the input port and isolation port, as well as the two output ports, must be kept perpendicular to each other. Since the coupler performance [21] is limited by port direction, fixed port angle interval makes it unsuitable for other port angular intervals topologies. Furthermore, all ports of the coupler are concentrated in an angle range of 135 degrees, which also leads to EMC problem. In particular, the traditional single type resonators [12-21] structure is not convenient to solve the problem that only part of the ports topology does not match with the desired direction, because it needs to maintain the consistency of the phase for each port. Therefore, the location of components connected to other ports also needs to be adjusted, which will further occupy additional circuit area and affect the overall layout of the system. In this paper, the proposed structures not only have relatively high Q factors, better isolation, simple structure, but also can be suitable for the application of multiple available port angle intervals (APAI), which is helpful to achieve high density and miniaturized RF/microwave wave system.

Table 1: Performance comparison of various filtering rat-race couplers

Ref.	f_0(GHz)/ FBW (%)/ε_r	IL (dB)/ Isolation (dB)/ Q factor	Mag.(dB)/ Phase(deg) Imbalance	APAI *	Circuit Size	Techniques/ Layers*/ Resonators*
[12]	2.4/10/2.2	0.7/20/80	1/2	1	$0.32\times0.32\lambda_g^2$	Microstrip/1/4
[13]	0.47/13/3.38	1.17/25/60	0.2/4.5	1	$0.23\times0.12\lambda_g^2$	Microstrip/1/8
[18]	20/2.6/2.2	1.63/28/190	0.3/5	1	$2.51\times2.51\lambda_g^2$	SIW/1/5
[19]	11/3.6/3.5	1.6/20/170	0.6/8	1	$1.59\times1.26\lambda_g^2$	SIW/1/4
[20]	7.75/2.7/3.5	1.5/25/200	0.6/5	1	$0.79\times0.45\lambda_g^2$	SIW/2/4
[21]	11.8/3.5/3.5	1.3/18/210	0.1/3	1	$1.18\times1.18\lambda_g^2$	SIW/1/3
This work	10.2/3.5/3.5	1.3/27/210	0.05/3	Multiple	$1.19\times1.19\lambda_g^2$	SIW/1/4
	10.28/2.5/3.5	1.38/30/210	0.1/3	Multiple	$1.16\times1.16\lambda_g^2$	SIW/1/4

Where λ_g is the guided wavelength on the substrate at the center frequency f_0, FBW represents the fractional bandwidth. APAI* represents the number of available port angular interval. Layers* represents the number of substrate layers. Resonators* represents the number of resonators.

V. CONCLUSION

In this paper, a novel type of compact band-pass rat-race couplers with flexible port direction based on mixed shape SIW cavities are proposed for the first time. Simulated and measured results have been presented to verify the proposed method. Based on a SIFC and three SIRCs, the other filtering rat-race coupler has been implemented for further verification. Generally, the proposed designs have shown excellent performance of filtering responses, isolation, amplitude balance, 0° and 180° phase differences, as well as the compact structure. In addition, the demand of circuit topology has been firstly integrated into design considerations. With flexible ports configuration but without deterioration of performance, the coupler's topology is easy to match with the desired transmission direction. The proposed filtering couplers with mixed resonators could be more suitable for the development of high density and miniaturized RF/microwave system.

ACKNOWLEDGMENT

This work was supported in part by the Ministry of Science and Technology of the People's Republic of China under Grant 2013YQ200503 and in part by the National Natural Science Foundation of China (NSFC) under Grant 61001028.

REFERENCES

[1] Y. Dong and T. Itoh, "Miniaturized dual-band substrate integrated waveguide filters using complementary split-ring resonators," *IEEE MTT-S Int. Microw. Symp. Dig*., pp. 1-4, June 2011.

[2] X.-P. Chen, K. Wu, and Z.-L. Li, "Dual-band and triple-band substrate integrated waveguide filters with Chebyshev and quasi-elliptic responses," *IEEE Trans. Microw. Theory Techn*., vol. 55, no. 12, pp. 2569-2578, Dec. 2007.

[3] K. Song and Q. Xue, "Novel ultra-wideband (UWB) multilayer slotline power divider with bandpass response," *IEEE Microw. Wirel. Compon. Lett*., vol. 20, no. 1, pp. 13-15, Jan. 2010.

[4] Y. J. Cheng, W. Hong, and K. Wu, "94 GHz substrate integrated monopulse antenna array," *IEEE Trans. Antennas Propag*., vol. 60, no. 1, pp. 121-128, Jan. 2012.

[5] Y. J. Cheng, W. Hong, K. Wu, and Y. Fan, "A hybrid guided-wave structure of half mode substrate integrated waveguide and conductor-backed slotline and its application in directional couplers," *IEEE Microw Wireless Compon Lett*. vol. 21, no. 2, pp. 65-67, Feb. 2011.

[6] Z.-G. Zhang, Y. Fan, Y. J. Cheng, and Y.-H. Zhang, "A compact multilayer dual-mode substrate integrated circular cavity (SICC) filter for X-band application," *Prog. Electromagn. Res*., vol. 122, no. 1, pp. 453-465, Jan. 2012.

[7] Z.-G. Zhang, Y. Fan, and Y.-H. Zhang, "Compact 3-D multilayer substrate integrated circular and elliptic cavities (SICCs and SIECs) dual-mode filter with high selectivity," *Appl. Comp. Electro. Society (ACES) Journal*, vol. 28, no. 4, pp. 333-340, Apr. 2013.

[8] Q. Chen and J. Xu, "Out-of-phase power divider based on two-layer SIW," *Electron Lett*., vol. 50, no. 14, pp. 1005-1007, July 2014.

[9] H. Uchida, N. Yoneda, and S. Makino, "Bandpass directional couplers with electromagnetically-coupled resonators," *IEEE MTT-S Int. Microwave Symp. Digest*. pp. 1563-1566, June 2006.

[10] L.-S. Wu, B. Xia, W.-Y. Yin, and J. Mao, "Collaborative design of a new dual-bandpass 180° hybrid coupler," *IEEE Trans. Microw. Theory Tech*., vol. 61, no. 3, pp. 1053-1066, Mar. 2013.

[11] P. Li, H. Chu, and R. S. Chen, "SIW magic-T with bandpass response," *Electron Lett*., vol. 51, no. 14, pp. 1078-1080, July 2015.

[12] C.-K. Lin and S.-J. Chung, "A compact filtering 180° hybrid," *IEEE Trans. Microw. Theory Tech*., vol. 59, no. 12, pp. 3030-3036, Dec. 2011.

[13] K.-X. Wang, X.-Y. Zhang, S.-Y. Zheng, and Q. Xue, "Compact filtering rat-race hybrid with wide stopband," *IEEE Trans. Microw. Theory Tech*., vol. 63, no. 8, pp. 2250-2560, Aug. 2015.

[14] J.-X. Xu, X.-Y. Zhang, and H.-Y. Li, "Compact narrowband filtering rat-race coupler using quad-mode dielectric resonator," *IEEE Trans. Microw. Theory Tech*., vol. 66, no. 9, pp. 4029-4039, Sep. 2018.

[15] L.-X. Jiao, Y.-L. Wu, Y.-N. Liu, and J.-X. Chen, "Concept for narrow-band filtering rat-race coupler using dual-mode cross-shaped dielectric," *Electron Lett*., vol. 52, no. 3, pp. 212-213, Feb. 2016.

[16] K.-X. Wang, X.-F. Liu, Y.-C. Li, L.-Z. Lin, and X.-L. Zhao, "LTCC filtering rat-race coupler based on eight-line spatially-symmetrical coupled structure," *IEEE Access*, vol. 6, no. 6, pp. 262-269, June 2018.

[17] Z.-G. Zhang, Y. Fan, and Y.-H. Zhang, "Multilayer half-mode substrate integrated waveguide wide-band coupler with high selectivity," *Appl. Comp. Electro. Society (ACES) Journal*, vol. 34, no. 9, pp. 1418-1425, Sep. 2019.

[18] S.-Q. Han, K. Zhou, J.-D. Zhang, C.-X. Zhou, and W. Wu, "Novel substrate integrated waveguide filtering crossover using orthogonal degenerate modes," *IEEE Microw. Wireless Compon. Lett*., vol. 27, no. 9, pp. 803-805, Sep. 2017.

[19] U. Rosenberg, M. Salehi, J. Bornemann, and E. Mehrshahi, "A novel frequency-selective power combiner/divider in single-Layer substrate integrated waveguide technology," *IEEE Microw Wireless Compon Lett*., vol. 23, no. 8, pp. 406-408, Aug. 2013.

[20] Y.-J. Cheng and Y. Fan, "Compact substrate-integrated waveguide bandpass rat-race coupler and its microwave applications," *IET Microw., Antennas Propag*., vol. 6, no. 9, pp. 1000-1006, June 2012.
[21] H.-Y. Li, J.-X. Xu, and X.-Y. Zhang, "Substrate integrated waveguide filtering rat-race Coupler based on orthogonal degenerate modes," *IEEE Trans. Microw. Theory Techn*., vol. 67, no. 1, pp. 140-150, Jan. 2019.
[22] M.-K. Li, C. Chen, and W. Chen, "Miniaturized dual-band filter using dual-capacitively loaded SIW cavities," *IEEE Microw. Wireless Compon. Lett*., vol. 27, no. 4, pp. 344-346, Apr. 2017.
[23] X. Zou, C.-M. Tong, C.-Z. Li, and W.-J. Pang, "Wideband hybrid ring coupler based on half-mode substrate integrated waveguide," *IEEE Microwave and Wireless Components Letters*, vol. 24, no. 9, pp. 596-598, Sep. 2014.
[24] S. Zhang, J.-Y. Rao, J.-S. Hong, and F.-L. Liu, "A novel dual-band controllable bandpass filter based on fan-shaped substrate integrated waveguide," *IEEE Microw. Wireless Compon. Lett*., vol. 28, no. 4, pp. 308-310, Apr. 2018.
[25] Y.-D. Dong and T. Itoh, "Miniaturized substrate integrated waveguide slot antennas based on negative order resonance," *IEEE Trans. Antennas Propag*., vol. 58, no. 12, pp. 3856-3864, Dec. 2010.
[26] M.-C. Tang, S. Q. Xiao, and D. Wang, "Negative index of reflection in planar metamaterial composed of single split-ring resonators," *Appl. Comp. Electro. Society (ACES) Journal*, vol. 26, no. 3, pp. 250-258, Mar. 2011.
[27] M.-C. Tang, H. Wang, L. Guo, X. P. Zeng, H. Liu, and Y. B. Pang, "A compact dual-band patch antenna design based on single-ring split ring resonator," *Appl. Comp. Electro. Society (ACES) Journal*, vol. 31, no. 3, pp. 321-326, Mar. 2016.
[28] Y. S. Li, W. X. Li, and W. H. Yu, "A switchable UWB slot antenna using SIS-HSIR and SIS-SIR for multi-mode wireless communications applications," *Appl. Comp. Electro. Society (ACES) Journal*, vol. 27, no. 4, pp. 340-351, Apr. 2012.
[29] R. Rezaiesarlak, M. Salehi, and E. Mehrshahi, "Hybrid of moment method and mode matching technique for full-wave analysis of SIW circuits," *Appl. Comp. Electro. Society (ACES) Journal*, vol. 26, no. 8, pp. 688-695, Aug. 2011.
[30] Z. J. Zhu, L. Cao, and C. L. Wei, "Novel compact microstrip dual-mode filters with two controllable transmission zeros," *Appl. Comp. Electro. Society (ACES) Journal*, vol. 33, no. 1, pp. 43-48, Jan. 2018.
[31] J.-S. Hong and M.-J. Lancaster, *Microstrip Filter for RF/Microwave Applications*. New York, NY, USA: Wiley; 2001.
[32] R.-J. Cameron, "Advanced coupling matrix synthesis techniques for microwave filters," *IEEE Trans. Microw. Theory Tech*., vol. 51, no. 1, pp. 1-10, Jan. 2003
[33] D.-M. Pozar, *Microwave Engineering*. 2nd edition, New York: Wiley; 1998.

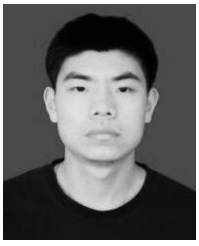

Zhigang Zhang was born in Shanxi Province, China. He received the B.S. degree in Electronic Information Engineering and M.S. degree in Wireless Physics from Sichuan University and is currently working toward the Ph.D. degree in Electro-magnetic Field and Microwave Technology from The University of Electronic Science and Technology of China (UESTC), Chengdu, Sichuan, China. His current research interests include SIW technology and its application, microwave and millimeter-wave filters and couplers, electromagnetic theory.

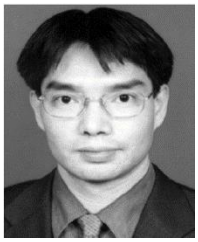

Yong Fan received the B.E. degree from the Nanjing University of Science and Technology, Nanjing, Jiangsu, China, in 1985, and the M.S. degree from the University of Electronic Science and Technology of China (UESTC), Chengdu, Sichuan, China, in 1992.

He fs currently with the School of Electronic Engineering, UESTC. He has authored or coauthored over 60 papers. From 1985 to 1989, he was interested in microwave integrated circuits. Since 1989, his research interests include millimeter-wave communication, electromagnetic theory, millimeter-wave technology, and millimeter-wave systems. Fan is a Senior Member of the Chinese Institute of Electronics (CIE).

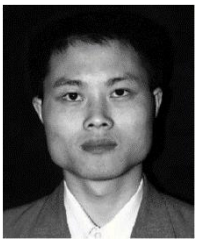

Yonghong Zhang received the B.S., M.S., and Ph.D. degrees from the University of Electronic Science and Technology of China (UESTC), Chengdu, China, in 1992, 1995, and 2001, respectively. From 1995 to 2002, he was a Teacher with the UESTC. In 2002, he joined the Electronic Engineering Department, Tsinghua University, Beijing, China, as a Doctoral Fellow. In 2004, he rejoined the UESTC. His research interests are in the area of microwave and millimeter-wave technology and applications.